International Journal of Pressure Vessels and Piping 146 (2016) 55–64

Contents lists available at ScienceDirect

International Journal of Pressure Vessels and Piping

journal homepage: www.elsevier.com/locate/ijpvp

Stress intensity interaction between dissimilar semi-elliptical surface cracks

H.E. Coules

Department of Mechanical Engineering, University of Bristol, Bristol, BS8 1TR, UK

ARTICLE INFO

Article history:
Received 11 January 2016
Received in revised form
27 July 2016
Accepted 27 July 2016
Available online 29 July 2016
Dedicated to the late Prof. David Smith

Keywords:
Stress intensity factor
Interaction
Semi-elliptical crack
Structural integrity assessment

ABSTRACT

Procedures for structural integrity assessment normally contain criteria to predict the significance of the interaction between neighbouring defects in a structure. Here, the elastic interaction between coplanar semi-elliptical surface cracks is examined in detail by considering a large number of dissimilar crack pairs with different depths and aspect ratios. Surface defect interaction criteria from several assessment procedures are critically assessed and found to be satisfactory for cracks loaded in uniform tension. The criterion used in the R6 Rev. 4 and BS 7910:2013 procedures is the least inherently conservative of those considered here. However, the amount by which interaction exacerbates the most severe crack front loading state can depend strongly on the distribution of stress applied to the cracks. This means that the loading mode should be taken into consideration when judging whether the interaction between surface defects is significant.

1. Introduction

In structural integrity analysis it is often necessary to predict the combined effect of two or more flaws in a structure. As a result, integrity assessment procedures such as the British assessment standard BS 7910:2013 [1], the R6 Rev. 4 procedure maintained by EDF Energy and others [2], and the ASME Boiler and Pressure Vessel Code Section XI [3] contain rules for analysing adjacent defects, in addition to guidance on how to predict their combined effect on a structure. These procedures are designed to cover various failure mechanisms including brittle fracture, elastic-plastic fracture and plastic collapse. However for simplicity and conservatism, rules for considering the interaction between adjacent defects are normally based on linear elastic fracture mechanics analyses. In practice this means determining how the stress intensity factor which occurs at one crack is influenced by the presence of an additional crack or defect close by.

The problem of interacting co-planar semi-elliptical surface cracks is a particularly important one because defects due to stress-corrosion cracking, fatigue, and weld cracking can often be approximated using this geometry. For co-planar surface defects, assessment codes typically provide rules for conservatively characterising the defects as semi-elliptical or rectangular cracks. Interaction criteria based solely on the defect geometry have been established using the results of numerical stress analyses in conjunction with the relatively scarce experimental data which exists for these cases [4–6].

The analysis of interacting cracks in a linear elastic material has developed steadily in response to improvements in capability for computational stress analysis. The most important early work on this problem used a 'body force' method of analysis based on equivalent Eshelby-type ellipsoidal inclusions [7,8]. This method is computationally efficient and allows analysis of a wide range of different crack sizes and aspect ratios, but it is best suited to analysis of cracks emanating from the free surface of an infinite half-space rather than cracks in plates and shells of finite thickness. Additionally, for materials with Poisson's ratios in a practical range (i.e. $\nu \approx 0.3$ for metals) it is difficult to derive accurate stress intensity factor results for points on the crack front close to an intersection with a free surface using the body force method [9]. The line-spring analysis developed by Rice and Levy [10] can be coupled with the boundary element method to yield results for semi-elliptical cracks. Zeng et al. [11] used this technique to analyse pairs of identical surface cracks, presenting a comparison between this and the crack pair re-classified as a single crack by the method given in ASME BVPC Section XI [3].

For cracks in finite-thickness plates with realistic elastic properties, the finite element method has proven to be a versatile technique despite entailing a greater computational cost than the

E-mail address: harry.coules@bristol.ac.uk.

http://dx.doi.org/10.1016/j.ijpvp.2016.07.011

body force and line-spring methods. Finite element results for interacting semi-elliptical cracks are presented by Soboyejo et al. [12], Stonesifer et al. [13] and Yoshimura et al. [14]; with the latter study in particular showing that FEA can be used to rapidly generate results for a large number of crack geometries. More recent finite element studies including those by Sethuraman et al. [15,16], and Carpinteri et al. [17] have used this method to determine stress intensity factors and interaction parameters for a range of semi-elliptical crack geometries. From this work, it is evident that the magnitude of the interaction between two cracks depends strongly on the distance between them and quickly becomes insignificant as this distance is increased [18]. Use of the finite element method also makes it practical to model crack growth and coalescence for processes such as fatigue which are driven by the stress field at the crack tip. Results from models of this type, modelling crack propagation from multiple initially semi-elliptical defects, have been presented in studies by Kishimoto et al. [19] and Lin & Smith [20].

So far, the majority of work on coplanar surface cracks has concentrated on studying the interaction between two identical defects. This greatly simplifies the problem of determining whether interaction between the cracks is significant enough to be considered in subsequent analysis. For a pair of dissimilar defects, there are far more possible combinations of crack depth and aspect ratio to be considered. Likewise, there has been a focus on the simplest defect loading modes: uniform tension and bending. In reality, non-linear variations in stress through the thickness of plates and shells frequently occur, often as a result of residual and thermal stresses. Although some researchers, such as Carpinteri et al. [17] have investigated the effects of these non-uniform loadings, interaction criteria typically do not include any dependence on loading mode.

The purpose of this study is to evaluate the criteria that are used within structural integrity assessment procedures to judge the significance of crack interaction effects. Using the results of finite element models of a broad range of dissimilar crack pairs, these criteria can be examined more thoroughly than when only data for pairs of identical defects is available. The effects of the through-thickness distribution of stress and the material's elastic properties on the effectiveness of interaction criteria have also been identified.

2. Stress intensity factor determination

2.1. Notation and conventions

Fig. 1 shows the basic geometry of a pair of dissimilar semi-elliptical defects emanating from the same surface on a plate of unit thickness. For convenience, the cracks are numbered 1 and 2. Crack 1 is always the deeper of the two if they have different depths (ie. $a_1 \geq a_2$) and is located positive in x relative to Crack 2. It is also convenient to parameterise the geometry of the crack pair using the following normalised factors: $\xi = a_1/b$ is the non-dimensional depth of Crack 1, $\beta = a_2/a_1$ is the depth of Crack 2 relative to Crack 1, $\alpha_1 = a_1/c_1$ is the aspect ratio of Crack 1, $\alpha_2 = a_2/c_2$ is the aspect ratio of Crack 2, and $\delta = d/b$ is the non-dimensional distance between the two cracks. For any pair of semi-elliptical cracks on the same side of a plate, $\xi < 1$, $\beta \leq 1$, $\alpha_1 > 0$, $\alpha_2 > 0$ and $\delta > 0$.

A point on either semi-ellipse can be defined using its parametric angle ϕ, as shown in Fig. 2. For each crack, ϕ is measured from the intersection point of the crack front with the plate surface closest to the other crack. This means that for cracks on the same side of the plate, Crack 1 has ϕ_1 measured anticlockwise-positive whereas for Crack 2, ϕ_2 is measured clockwise-positive.

To examine the interaction of the two cracks, an interaction factor γ can be defined as [17]:

$$\gamma(\phi) = \frac{K_I^{int}(\phi)}{K_I^{\delta=\infty}(\phi)} \tag{1}$$

where K_I^{int} is the Mode I stress intensity factor at the interacting crack and $K_I^{\delta=\infty}$ is the Mode I stress intensity factor for a crack of the same geometry and under the same loading conditions, but remote from any other defect. Since the Mode I stress intensity factor for each crack varies as a function of position over the crack front, γ is a function of ϕ. Examples showing the variation in $\gamma(\phi)$ across the crack front in pairs of identical cracks are given in Section 3.1 (Figs. 4 and 5). However, in general Crack 1 and Crack 2 may have differing depths and aspect ratios, and consequently they may have differing interaction factor functions. These can be written as:

$$\gamma^N(\phi) = \frac{K_I^{N,int}(\phi)}{K_I^{N,\delta=\infty}(\phi)} \tag{2}$$

where the superscript N may take the value 1 or 2 to indicate values for Crack 1 and Crack 2 respectively. For example $K_I^{2,\,int}$ denotes the Mode I stress intensity factor on Crack 2 when it is in proximity to the other crack. For assessing whether or not the interaction between two cracks is significant it is useful to further define a 'global' interaction factor γ^G. This is the factor by which the maximum Mode I stress intensity factor present anywhere on either crack line is increased by proximity of the cracks to one another:

$$\gamma^G = \frac{\max\limits_{\phi,N} K_I^{N,\,int}(\phi)}{\max\limits_{\phi,\,N} K_I^{N,\,\delta=\infty}(\phi)} \tag{3}$$

This quantity represents the amount by which the most unfavourable condition on the crack pair (according to single-parameter linear elastic fracture mechanics) has been exacerbated by interaction between the cracks.

2.2. Finite element analysis

The Abaqus/CAE finite element pre-processor [21] working in conjunction with custom code written in MATLAB [22] and Python was used to automatically generate individual finite element models for a large number of different crack pairs. For each crack pair, model geometry information including the crack positions, mesh transition positions, element sizes etc. was defined using the basic parameters ξ, β, α_1, α_2 and δ (defined in Section 2.1). This geometric information was written into a Python script specifying the process required to generate a model via the Abaqus/CAE scripting interface. The script was executed, causing Abaqus/CAE to create and mesh a model, and write an input file which could be passed to the FE solver. All of the analyses were performed using the Abaqus/Standard 6.12 solver [23] on a server machine with 12 Intel Xeon ×5670 CPUs and 50 GB of RAM running under CentOS Linux 6.8. Further MATLAB code was used to control the execution of models and extract results from the output files.

Since the solid body is symmetric about the plane containing the cracks, it is only necessary to model one half of it. The nominally infinite plate containing the cracks was approximated using a finite plate which was large in comparison to the region containing the cracks: 1000 × 1000 units in breadth and half-length for a plate of unit thickness. Three types of mesh generation region were used. The crack tip region (Region 1) consists of 8-noded reduced integration linear brick elements arranged in a layer five elements thick, which surround a set of 6-noded linear wedge elements at the crack tip. 50 elements were used along the length of each semi-

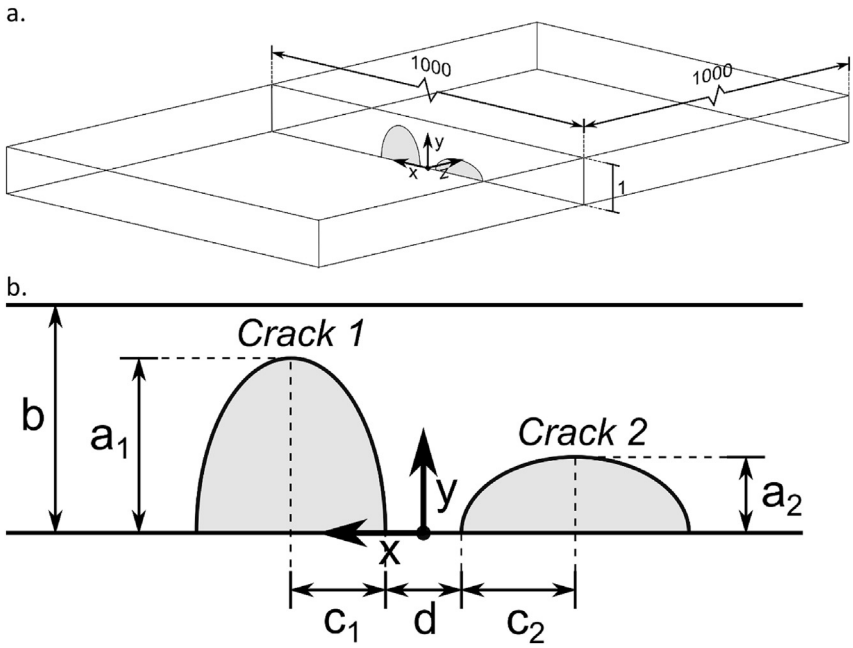

Fig. 1. Dissimilar semi-elliptical defects in a plate of finite thickness. a.) Schematic diagram of the complete plate (not to scale). b.) Region containing semi-elliptical defects.

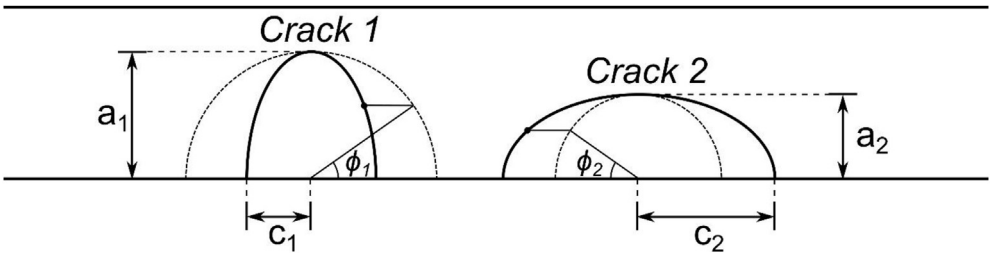

Fig. 2. Defining points on the crack front using the ellipse parametric angle ϕ.

elliptical crack front. The cracks were embedded in a region of 10-noded quadratic tetrahedron elements (Region 2) to allow models with wide geometric variation to be meshed automatically. Tie constraints were used to couple this region to the rest of the model. Finally, the remaining part of the model is meshed using 8-noded reduced integration linear bricks to allow an efficient, structured mesh to be used for this much larger volume (Region 3).

Loading was applied as an equivalent crack face pressure [24]. For example, a uniform pressure normal to the crack face was used to produce crack front loading equivalent to a state of uniform remote tension. Mode I stress intensity factors for each position along each crack tip were extracted from the resulting stress field by calculating the J-integral and using the interaction integral method to extract K_I [25]. Sensitivity studies using selected crack geometries were performed to verify that the level of mesh refinement was sufficient for accurate determination of the stress field. Additional checks were carried out on all models to ensure that the contour integral results were path-independent. An example showing the automatically generated mesh surrounding the crack region, and a stress field calculated using it, can be seen in Fig. 3. In this example the generated mesh comprises 73,487 solid elements, the material has Poisson's ratio $\nu = 0.3$, and the crack geometric parameters are: $\xi = 0.75$, $\beta = 0.5$, $\alpha_1 = 2$, $\alpha_2 = 0.5$ and $\delta = 0.25$.

In materials with $\nu \neq 0$, the strength of the stress singularity at the intersection points between the crack front and the free surface of the plate deviates from $r^{-½}$ by a small amount [26–28]. This creates a boundary layer close to the free surface in which the apparent stress intensity factor is reduced [28]. However, in this study the effect of the free surface singularity on the subsequent analysis is not considered. The interaction factor results, which are ratios rather than absolute values of K_I, were observed to vary smoothly with ϕ close to the free surface. Since the subsequent discussion focusses on interaction factor, effects relating to the presence of the free surface are unlikely to influence the analysis.

2.3. Parameter space

A large number of crack pair geometries were analysed using the method described in Section 2.2. Pairs of semi-elliptical surface cracks were defined using every combination of the geometric parameters listed in Table 1: a total of 7350 crack pairs.

Using this geometry set, analyses were performed with different crack loading conditions and for materials with different values of Poisson's ratio. The loading conditions were defined in terms of a through-thickness distribution to stress normal to the crack plane $\sigma_{zz}(y/b)$. Stress distributions defined by:

$$\sigma_{zz_n}\left(y/b\right) = \left(y/b\right)^n \; n = 0, \ldots, 5 \tag{4}$$

were used. As a weighted sum, these elementary stress

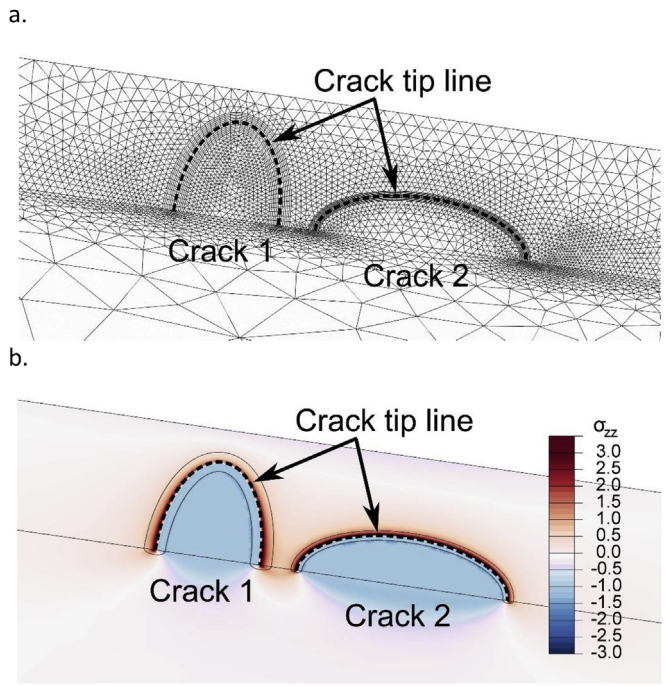

Fig. 3. Finite element mesh generation and model solution. a.) Automatically generated mesh for the crack region. b.) The stress field (σ_{zz} component shown) resulting from a uniform crack face pressure of unit magnitude.

stress distribution:

$$K_I(\phi) = \sum_{n=0}^{5} A_n K_{I_n}(\phi) \tag{6}$$

where $K_{I,n}$ is the Mode I stress intensity factor resulting from crack loading by a stress distribution $\sigma_{zz,n}(y/b)$ as defined in Equation (4). This method of decomposing the through-thickness stress distribution is used extensively within the R6 procedure [2]. Results for these different loading cases were calculated for a material with $\nu = 0.3$ only. However, for the case of uniform tension ($n = 0$) analyses were also performed for materials with $\nu = 0.2$ and $\nu = 0.4$. This is summarised in Table 2. The 7350 geometric cases (Table 1) and eight sets of material and loading parameters (Table 2) resulted in 58,800 separate finite element simulations. Additional simulations were performed to determine stress intensity factor distributions for single cracks of various sizes and aspect ratios under the conditions given in Table 2 so that interaction factors could be calculated. Finally, in addition to the main set of analyses smaller parameter sets were used to replicate cases studied previously by Yoshimura et al. [14] and Sethuraman et al. [16] for the purpose of comparison.

3. Results and discussion

3.1. Comparison with existing results

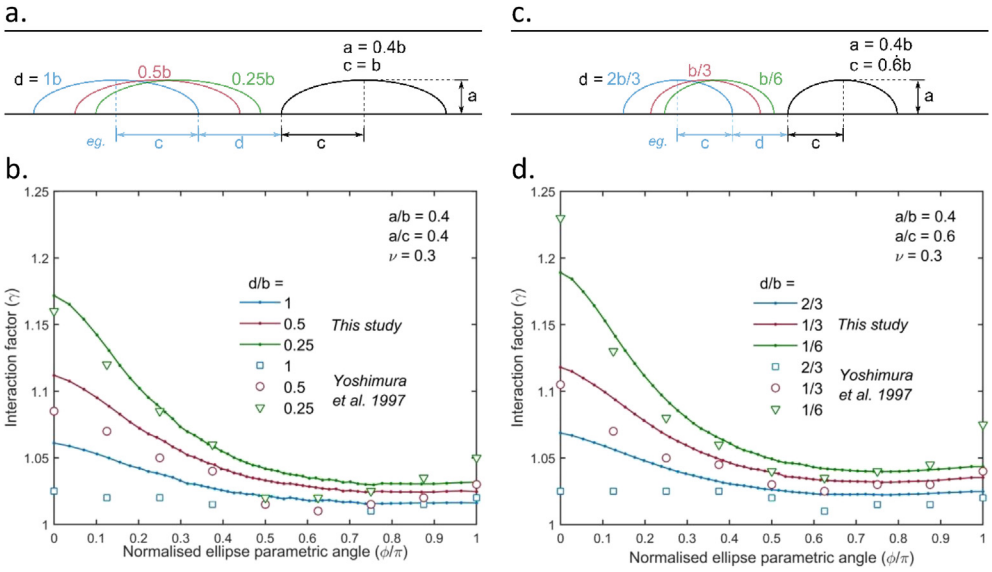

Fig. 4. Pairs of identical cracks under uniform tension analysed by Yoshimura et al. [14] and comparison with results of the present study. a. & b.) Pairs of cracks with a depth of $a/b = 0.4$ and aspect ratio of $a/c = 0.4$. c. & d.) Pairs of cracks with a depth of $a/b = 0.4$ and aspect ratio $a/c = 0.6$.

distributions can be used to represent a polynomial through-thickness distribution of stress [29,30],:

$$\sigma_{zz}\left(y/b\right) = \sum_{n=0}^{5} A_n \sigma_{zz_n}\left(y/b\right) \tag{5}$$

where A_n is a coefficient representing the contribution of each elementary term to the overall stress state. Likewise, stress intensity factor results for these different loading conditions can be combined to produce results for a polynomial through-thickness

There is very little published data dealing with the interaction of dissimilar semi-elliptical cracks in finite-thickness plates, however some data is available for pairs of identical cracks. For example, in the studies by Yoshimura et al. [14] and Sethuraman et al. [16] the variation in interaction factor over the crack tip is given for a number of cases involving pairs of identical semi-elliptical defects. Figs. 4 and 5 show several crack geometries for which interaction factor data are presented in these previous studies, and which have been re-analysed in the present work. For all of these cases, $\nu = 0.3$ and the loading condition is uniform tension in the direction

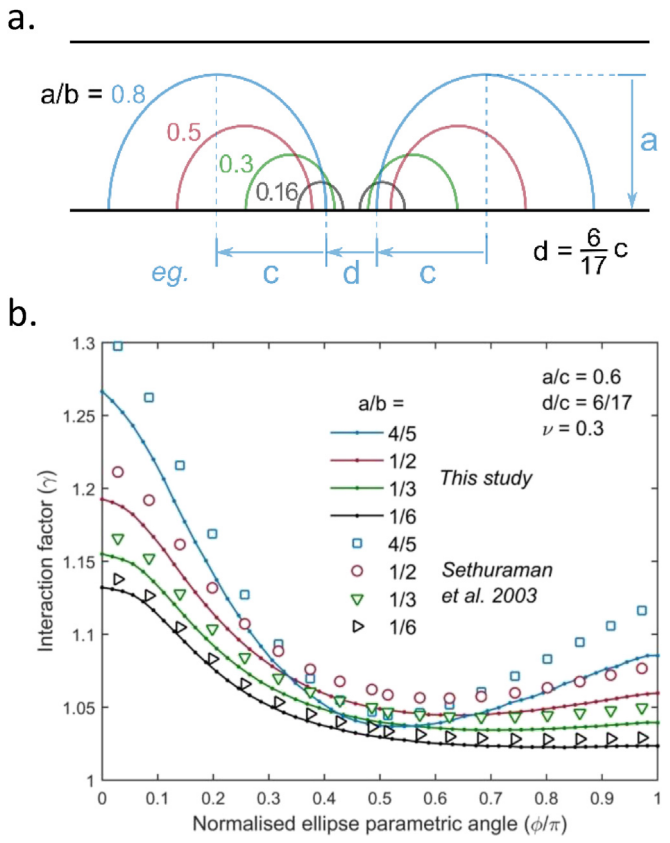

Fig. 5. Interaction factor under uniform tension as a function of ellipse parametric angle for pairs of identical cracks with aspect ratio $a/c = 1.2$, and comparison with the results of Sethuraman et al. [16]. a.) Four pairs of identical cracks, b.) interaction factor over the crack front as a function of ellipse parametric angle.

Table 1
Geometric parameters for pairs of semi-elliptical cracks on a plate. All combinations of these parameters were used to produce the main set of crack pair geometries.

Parameter	Values	No. Values
ξ	0.125, 0.25, 0.5, 0.75, 0.875	5
β	0.25, 0.3•, 0.5, 0.75, 0.8750, 1	6
α_1	0.4, 0.5, 0.6•, 1, 1.5, 2, 2.5	7
α_2	0.4, 0.5, 0.6•, 1, 1.5, 2, 2.5	7
δ	0.0625, 0.125, 0.25, 0.5, 1	5
	Total combinations:	*7350*

Table 2
Combinations of through-thickness stress distribution and Poisson's ratio for which semi-elliptical cracks on the same side of a finite-thickness plate were analysed.

Parameter set #	ν	n
1	0.3	0
2	0.3	1
3	0.3	2
4	0.3	3
5	0.3	4
6	0.3	5
7	0.2	0
8	0.4	0

normal to the crack plane.

In both cases there is general agreement in terms of interaction factor variation over ϕ between this study and the preceding results; but this correspondence is not exact. The interaction factor for each point along the crack line is calculated using two numerically-determined values of Mode I stress intensity factor (see Equation (1)), and therefore errors in K_I determination are propagated through to the calculated value of γ. However, none of the interaction factor results presented for this study differ from those given by Yoshimura et al. and Sethuraman et al. by more than 5%. Given the approximate nature of the calculation method used in all three studies (the finite element method), this indicates that there is overall agreement between the results of this study and previous results for interacting cracks, and that the results presented here are sufficiently accurate for most purposes.

Of the 7350 crack pairs in the main parameter space (Table 1), approximately 6% could not be analysed automatically using the technique described in Section 2.2. A summary of the completed and failed analyses for cracks under uniform tension in a material with $\nu = 0.3$ is shown in Table 3. The main cause of failed analyses was that for some geometries in which the cracks were situated extremely close together, it was not possible to generate a crack tip mesh region of sufficient size to ensure reliable contour integral results. Almost all models where meshing failed (98%) were for crack pairs with $\delta = 0.0625$, i.e. the smallest crack separation considered.

3.2. Assessment of crack interaction criteria: uniform tension

Four criteria for surface defect interaction have been compared: the first is used in both R6 Rev. 4 [2] and BS 7910:2013 [1], the second appears in the ASME B&PV Code Section XI [3] and the Japanese assessment code JSME S NA1 [31], the third is used in the joint API 579-1/ASME Fitness-For-Service assessment guidelines [32], while the fourth is used in the Chinese assessment standard GB/T 19624-2004 [33] and in Swedish assessment procedure SSM 2008:01 [34]. Both the R6 Rev. 4 and BS7910:2013 assessment procedures use the following geometric criterion to determine whether two coplanar semi-elliptical surface defects interact significantly [1,2],:

$$d \le \min(2c_1, 2c_2) \quad for \quad \frac{a_1}{c_1} > 1 \ \ or \ \ \frac{a_2}{c_2} > 1$$

$$d \le \max\left(\frac{a_1}{2}, \frac{a_2}{2}\right) \quad for \quad \frac{a_1}{c_1} \le 1 \ \ and \ \ \frac{a_2}{c_2} \le 1 \tag{7}$$

If these inequalities are satisfied then the defects are considered to interact, and must be re-characterised as a larger crack enclosing both defective areas. By comparison, the ASME Boiler and Pressure Vessel Code Section XI uses the following criterion, identical to the second expression in Equation (7) [3]:

$$d \le \max\left(\frac{a_1}{2}, \frac{a_2}{2}\right) \tag{8}$$

Defects with an aspect ratio of $a/c > 1$ are not considered acceptable under the ASME code and so no criterion for determining interaction for cracks of high aspect ratio (as in the first

Table 3
Summary of results status for models of crack pairs in the main parameter space under uniform tension.

R6 classification	FEA results	Number of cases
Classified as interacting	Yes	3442
	No	379
Classified as non-interacting	Yes	3478
	No	51
	Total	7350

expression in Equation (7)) is required [3,35]. An important distinction is that under the ASME code, defects are initially characterised as rectangular planar cracks, while under the R6 Rev. 4 and BS 7910:2013 procedures they can be characterised as an enclosing semi-elliptical crack. The API 579-1 procedure uses the criterion [32]:

$$d \leq c_1 + c_2 \tag{9}$$

However, this is not applied to flaws with a depth ratio greater than $\xi = 0.8$, which are characterised as through-wall cracks rather than semi-ellipses. Finally, the Chinese GB/T 19624-2004 assessment standard uses [33]:

$$d \leq 2c_2 \tag{10}$$

Like the criterion from API 579-1, this is only applied to defect pairs with a maximum depth below a critical value: individual defects with a deep ratio greater than $\xi = 0.7$ are instead characterised as through-wall cracks. Furthermore, the individual defect characterisation rules for fracture assessment in GB/T 19624-2004 ensure that when surface defects are characterised by a semi-ellipse, it always has an aspect ratio of $\alpha \leq 1$. The Swedish assessment procedure SSM 2008:01 [34] uses a criterion which is essentially the same as that found in GB/T 19624-2004 but without a limit on depth ratio ξ, so this procedure will not be individually discussed.

The R6/BS 7910 criterion is the most detailed of the four methods outlined above, and so will be considered first. All of the geometric cases in the main parameter space defined in Table 1 were first classified according to R6/BS 7910 as either 'interacting' or 'non-interacting'. For each crack geometry, the interaction classification was compared with interaction factor results calculated for a material with $\nu = 0.3$ under uniform remote tension (i.e. Case #1 in Table 2). Although in Section 2.3 no attempt was made to ensure that the set of crack pair geometries used covered the parameter space in an even or statistically unbiased manner, this comparison makes it easy to identify cases where a crack pair with a high interaction factor is classified as non-interacting, i.e. where there has been a potentially non-conservative classification.

The histograms in Fig. 6 show the proportion of crack pairs which were classified as non-interacting by the R6/BS 7910 criterion against their actual interaction factors calculated using finite element analysis. Taking the first line point and histogram bar in Fig. 6a as an example, 2872 crack pairs were determined to have an interaction factor of $1 \leq \gamma < 1.025$ at $\phi = 0$ on Crack 1, of which 84.8% would be classified as 'non-interacting' under R6/BS 7910. It is apparent that many of the geometries classified as 'non-interacting' do in fact show significant interaction at these surface points. However, although these points of closest approach between cracks typically have the greatest interaction factors, in most cases they present a lower absolute value of K_I than can be found elsewhere on the crack front, for example at the deepest point on the crack.

The global interaction factor (Equation (3)) gives a better appreciation of how interaction between the cracks exacerbates the most severe condition on either crack front, and is shown in Fig. 7a. By this measure of interaction the R6 criteria work well: few cases with a large global interaction factor are classified as non-interacting, which implies that there is a low risk of a non-conservative classification. At the same time, the majority of crack pairs with $\gamma^G < 1.025$ are correctly identified as not having significant interaction. All of the cases classified as non-interacting under the R6/BS7910 criteria which actually have a global interaction factor of $\gamma^G \geq 1.2$ involve very deep cracks with $\xi = 0.875$.

The remaining three histograms in Fig. 7 show the distribution of crack pairs as classified under the criteria set out in the ASME B&PV, API 579-1 and GB/T codes. Unlike in R6/BS 7910, under the ASME procedure shown in Fig. 7b certain crack pairs (i.e. those with high aspect ratio cracks) would not be classified using surface defect interaction criteria, and are therefore shown as 'unclassified'. However, compared with R6/BS 7910 the ASME procedure is equally conservative in assessing the significance of interaction between surface defects for cases where such classification is required by the procedure. The API 579-1 criterion can be used to classify a greater proportion of the crack pairs (see Fig. 7c), but is rather more conservative than either the R6/BS 7910 or the ASME B&PV procedures. Finally, the GB/T 19624-2004 standard has quite stringent rules for single flaw characterisation, and consequently many of the crack pairs considered here would not be examined under the GB/T 19624-2004 interaction rules. The interaction criterion used in GB/T 19624-2004 is also quite conservative: only a small minority of the crack pairs considered would be assessed as not interacting significantly.

Only the effect that crack interaction has on the Mode I stress intensity factor has been considered here: for simplicity, the effect of interaction on crack front constraint and on cracks in elastic-plastic materials is not discussed. Depending on the mechanism of failure these factors may be significant, and so may also be considered when formulating defect interaction criteria. Also, within the context of purely elastic analysis all defect pairs will interact to some degree. The level at which this interaction can be deemed significant for the purpose of structural integrity assessment is a matter of engineering judgement. Therefore, although results such as those shown in Fig. 7 are useful for comparing interaction criteria, they do not determine the required level of conservatism in such criteria.

3.3. The effect of Poisson's ratio and the through-thickness distribution of stress

The effect of Poisson's ratio on elastic crack interaction was studied by analysing dissimilar cracks in plates under uniform tension for materials with $\nu = 0.2$ (Case #7 in Table 2), $\nu = 0.3$ (Case #1) and $\nu = 0.4$ (Case #8). Most structural materials have a Poisson's ratio within this range. For each value of Poisson's ratio, 7350 crack pairs were analysed and the global interaction factor for each crack pair and each value of ν was calculated according to Equation (3). For the materials with $\nu = 0.2$ and $\nu = 0.4$ the following global interaction factor ratio was calculated:

$$\Gamma = \frac{\gamma_G}{\gamma_G^{ref}} \tag{11}$$

where γ_G is the global interaction factor for the crack pair in a particular material, and γ_G^{ref} is the corresponding global interaction factor for a reference condition; in this case for the same crack pair in a material with $\nu = 0.3$ under uniform tension. The distribution of crack geometries according to their Γ ratio at $\nu = 0.2$ and $\nu = 0.4$ is shown in Fig. 8.

All of the crack pairs at both values of ν have global interaction factor ratios $0.9 < \Gamma < 1.1$, indicating that variations in Poisson's ratio in the range $0.2 \leq \nu \leq 0.4$ only weakly influence the most severe loading condition which occurs in the crack pair. An example demonstrating the effect of differences in Poisson's ratio on the interaction between a pair of dissimilar cracks is shown in Fig. 9. The Poisson's ratio of the material has only a weak effect on the stress field surrounding the cracks, and hence on the stress intensity and interaction factor results. Consequently, the discussion of different interaction criteria given in Section 3.2 can be generalised to cover all linear elastic and isotropic materials with

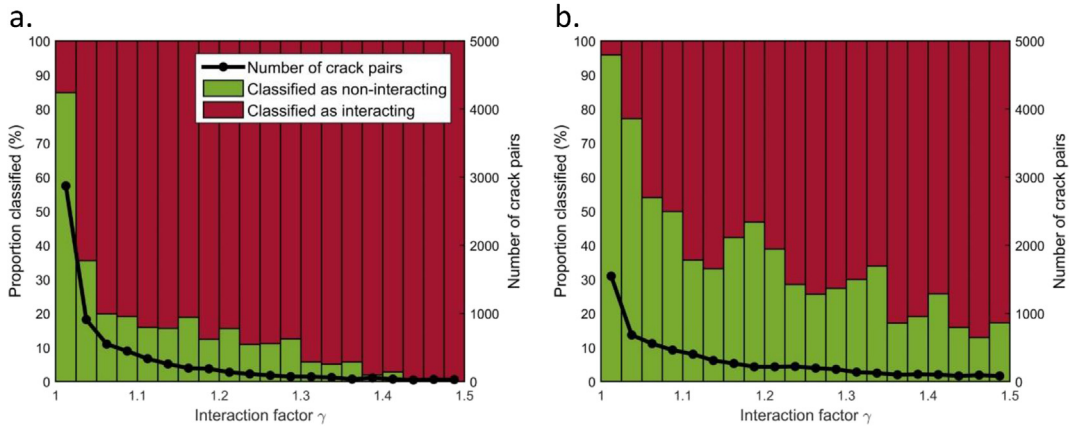

Fig. 6. Distribution of crack pair cases (n = 6920) by their interaction factor for a material with $\nu = 0.3$ under uniform tension, and their interaction classifications according to the R6/BS 7910 criterion. a.) According to interaction factor at $\phi = 0$ on Crack 1, b.) According to interaction factor at $\phi = 0$ on Crack 2.

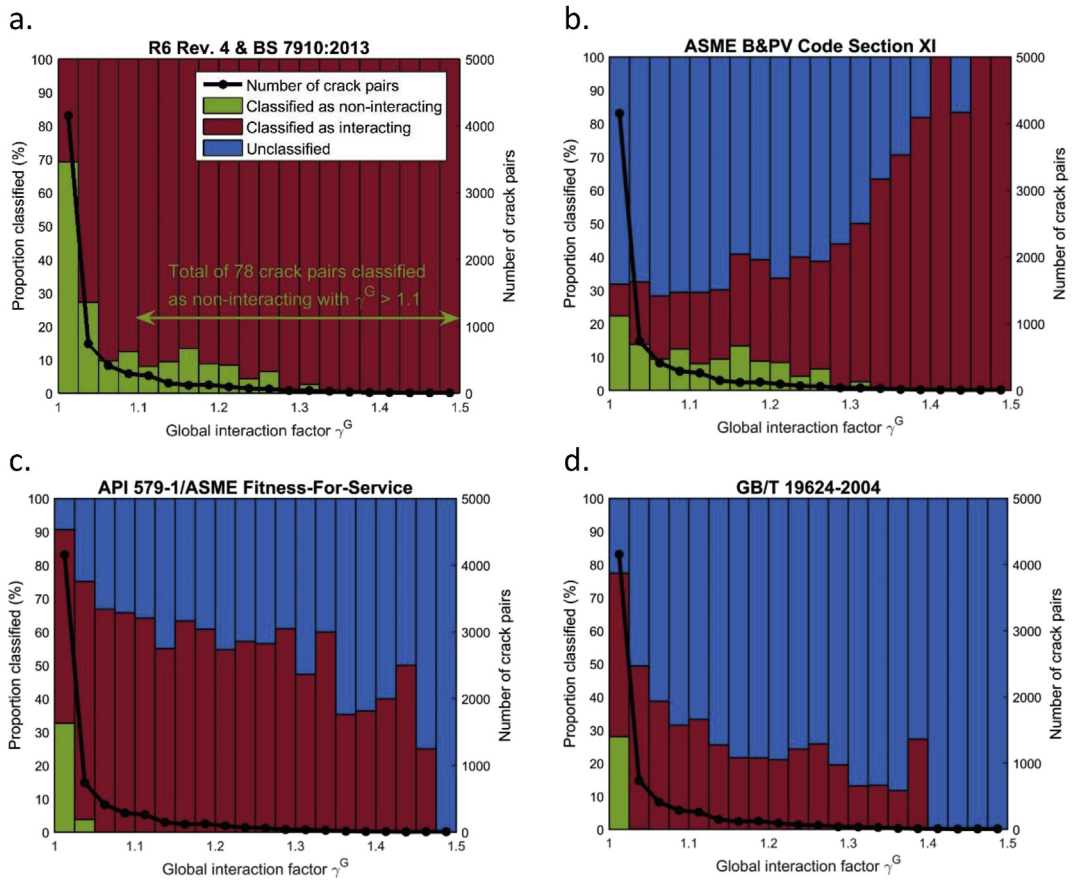

Fig. 7. Distribution of crack pairs (n = 6920) by their global interaction factor for a material with $\nu = 0.3$ under uniform tension, and their interaction classifications according to four criteria used in different integrity assessment procedures: a.) R6 Rev. 4 and BS 7910:2013, b.) ASME B&PV Code Section XI, c.) API/ASME 579-1 Fitness-For-Service, d.) Chinese assessment standard GB/T 19624-2004.

$0.2 \leq \nu \leq 0.4$.

A set of six elementary through-thickness stress distributions is defined by Equation (4) and the analyses performed to study the effect of these are outlined in Table 2 (Cases #1–6). By combining stress intensity factor results for these elementary distributions, the effect of many different through-thickness loading conditions on crack interaction was examined. The through-thickness distribution of stress applied to the crack pair can have a pronounced effect on the interaction factor. Fig. 10 shows the interaction factor as a function of position on the crack front for the dissimilar crack pair shown in Fig. 9a under the six elementary loading conditions. It can be seen that the loading mode affects the interaction factor dramatically at some points on the crack fronts.

For many crack pairs, the loading mode also affects the global interaction factor significantly. As an example, the global interaction factor was calculated for all of the crack pairs under the action

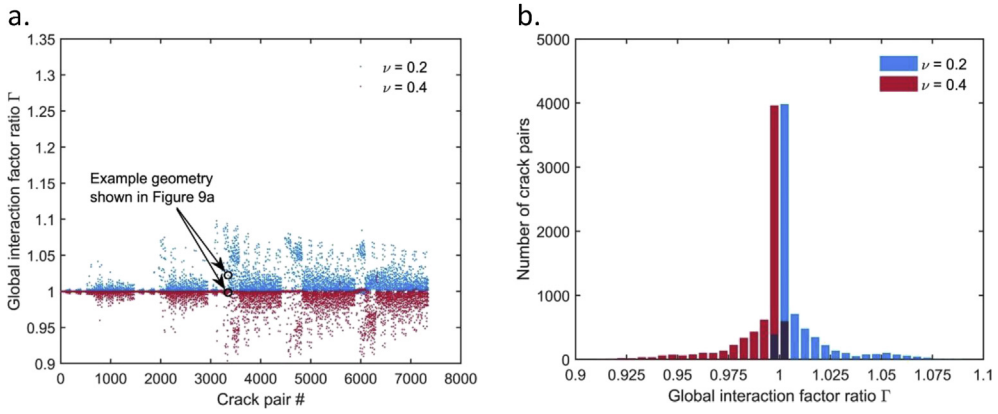

Fig. 8. Distribution of the global interaction factor ratio Γ for two sets of 6920 crack pairs in materials with different values of Poisson's ratio. a.) Individual crack pairs according to their Γ value. b.) Frequency distribution of Γ.

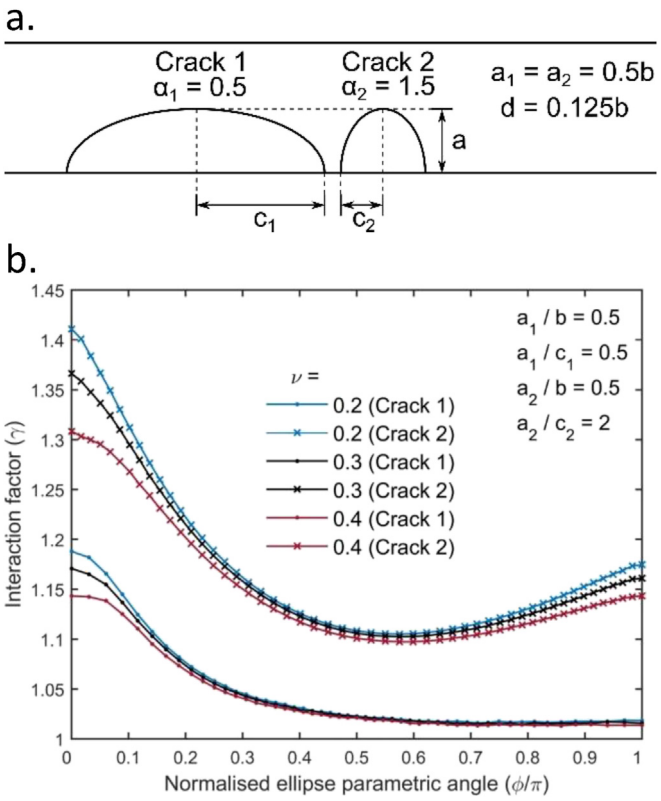

Fig. 9. Example showing the effect of Poisson's ratio on the interaction between a pair of dissimilar cracks. a.) Crack pair geometry, b.) interaction factor as a function of location on the crack front for three values of Poisson's ratio.

of the following through-thickness stress distribution:

$$\sigma_{zz}\left(\frac{y}{b}\right) = 0.9415 - 0.0319\left(\frac{y}{b}\right) - 8.3394\left(\frac{y}{b}\right)^2 + 8.660\left(\frac{y}{b}\right)^3 \quad (12)$$

The R6 procedure contains a compendium of stress distributions which may be used to represent the residual stress in welded components when the actual stress distribution is unknown. Equation (12) is used to represent the stress component transverse to a linear plate butt weld in austenitic or ferritic steel, normalised to the material's yield stress [2]. The ratio of the global interaction factor under this loading condition to the global interaction factor under uniformly tensile loading was calculated according to Equation (11) and the results plotted in Fig. 11. It is more than 1.3 for some cases, demonstrating that the loading mode can strongly affect the amount by which interaction exacerbates the most severe crack tip loading condition in the crack pair.

Fig. 12 shows the distribution of crack pairs according to their global interaction factor under the loading described by Equation (12). It can be compared directly with Fig. 7a, which is plotted for uniform tension loading. Under the Equation (12) loading condition, 139 crack pairs which have $\gamma_G > 1.1$ are classified as 'non-interacting' by the R6/BS 7910 criterion, compared with just 78 for uniform tension loading. This indicates that the effect of a non-uniform through-thickness stress distribution may introduce unintended non-conservatism into the judgement of whether interaction between surface defects is significant.

4. Conclusions

The interaction between co-planar semi-elliptical cracks of differing size and aspect ratio in an elastic plate has been examined. In many cases, cracks pairs which would be classified as having negligible interaction effects under the interaction criteria used in the R6 Rev. 4 and BS 7910:2013 assessment procedures do, in fact, interact (see Fig. 6). However in the vast majority of these cases, the greatest value of K_I on the crack front is not increased significantly: interaction mainly affects regions of the crack front which are less severely loaded. Consequently the R6/BS 7910 criterion performs well for determining when defect interaction would affect a structural integrity assessment significantly, even for interaction between defects with very different sizes and aspect ratios. The criteria used in the ASME Boiler and Pressure Vessels Code Section XI, API 579-1/ASME Fitness-For-Service and the Chinese assessment standard GB/T 19624-2004 are also satisfactory, but generally more conservative.

The level of elastic interaction that occurs between a pair of cracks depends on the distribution of stress that acts on them. Defect interaction criteria used in current integrity assessment procedures are independent of loading mode, and in some cases there is a risk of non-conservative interaction classification if through-thickness loading effects are overlooked. On the other hand, variation in Poisson's ratio in the range $0.2 \leq \nu \leq 0.4$ has only a weak effect on elastic interaction between surface cracks, which justifies the use of interaction criteria which are independent of material elastic properties.

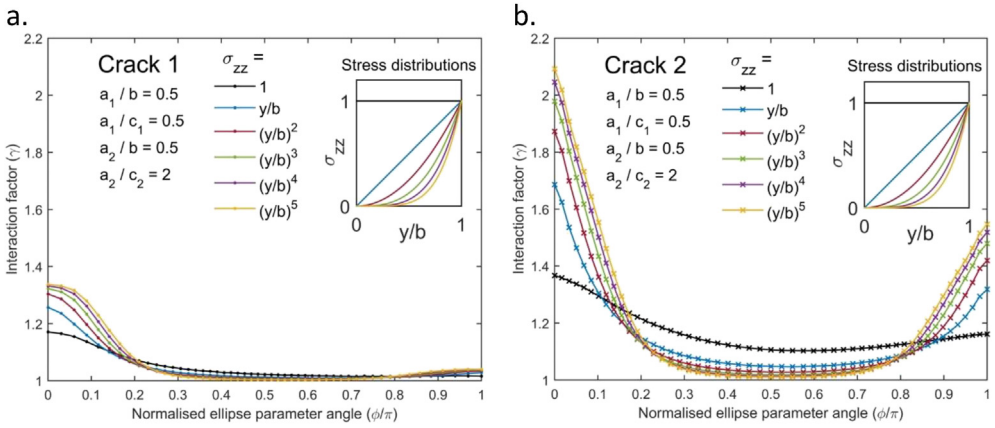

Fig. 10. Interaction factor as a function of crack front location for the crack pair shown in Fig. 9a under different out-of-plane loading conditions with $\nu = 0.3$. a.) Crack 1, b.) Crack 2. Inset shows the stress distribution for each loading condition.

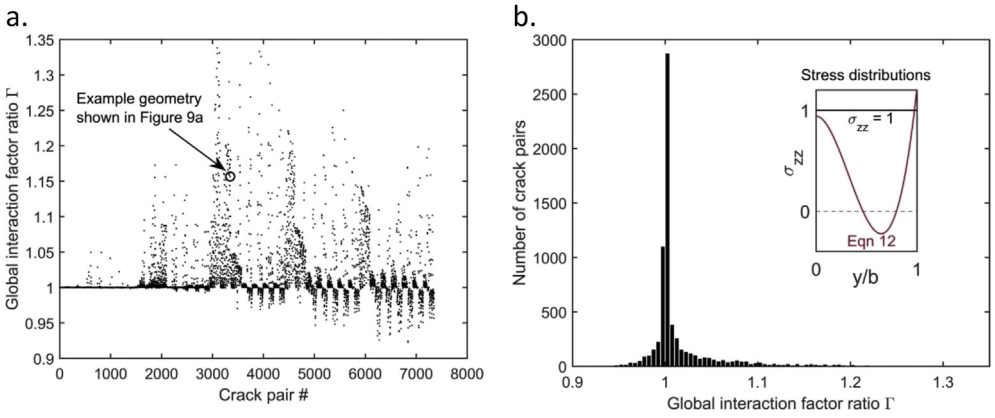

Fig. 11. Distribution of the global interaction factor ratio Γ for 6851 crack pairs acted on by the through-thickness distribution of stress defined by Equation (12). The reference condition (see Equation (11)) is uniformly tensile loading. a.) Individual crack pairs according to their Γ value. b.) Frequency distribution of Γ, inset shows loading conditions.

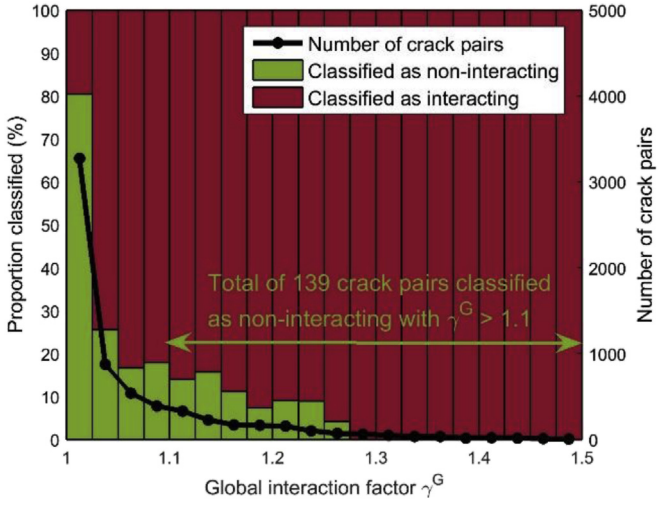

Fig. 12. Distribution of crack pairs (n = 6851) by their global interaction factor for a material with $\nu = 0.3$ subject to the stress distribution in Equation (12), and their interaction classifications according the R6 Rev. 4/BS 7910:2013 criterion.

Acknowledgements

The author is indebted to Dr Peter Budden for several interesting discussions relating to this study. The work was supported by the UK Engineering and Physical Sciences Research Council under grant no. EP/M019446/1 “Advanced structural analysis for the UK nuclear renaissance”.

Supplementary data

Results for all of the crack pair geometries examined in this study are available in MATLAB. mat format via the following link: http://dx.doi.org/10.5523/bris.wemj6fzqe5b61n2azn5f7jaxy.

References

[1] BS 7910:2013-Guide to methods for assessing the acceptability of flaws in metallic structures. BSi; 2013.
[2] R6: assessment of the integrity of structures containing defects, revision 4, amendment 10. Gloucester, UK: EDF Energy; 2013.
[3] 2013 ASME boiler and pressure vessel code section XI. New York, NY, USA: American Society of Mechanical Engineers; 2013.
[4] Azuma K, Li Y, Hasegawa K. Evaluation of stress intensity factor interactions between adjacent flaws with large aspect ratios. In: Proceedingsof the ASME pressure vessels and piping conference; 2015. no. 45063.
[5] Bezensek B, Sharples J, Hadley I, Pisarski H. The history of BS7910 flaw interaction criteria. In: Proceedings of the ASME pressure vessels and piping division conference; 2011. no. 57857.
[6] Leek TH, Howard IC. An examination of methods of assessing interacting

surface cracks by comparison with experimental data. Int J Press Vessels Pip 1996;68(2):181–201.
[7] Murakami Y, Nemat-Nasser S. Interacting dissimilar semi-elliptical surface flaws under tension and bending. Eng Fract Mech 1982;16(3):373–86.
[8] Nisitani H, Murakami Y. Stress intensity factors of an elliptical crack or a semi-elliptical crack subject to tension. Int J Fract 1974;10(3):353–68.
[9] Noda N-A, Kobayashi K, Oohashi T. Variation of the stress intensity factor along the crack front of interacting semi-elliptical surface cracks. Arch Appl Mech 2001;71(1):43–52.
[10] Rice JR, Levy N. The part-through surface crack in an elastic plate. J Appl Mech Trans ASME 1972;39(1):185–94.
[11] Zeng Z-J, Dai S-H, Yang Y-M. Analysis of surface cracks using the line-spring boundary element method and the virtual crack extension technique. Int J Fract 1993;60(2):157–67.
[12] Soboyejo WO, Knott JF, Walsh MJ, Cropper KR. Fatigue crack propagation of coplanar semi-elliptical cracks in pure bending. Eng Fract Mech 1990;37(2):323–40.
[13] Stonesifer RB, Brust FW, Leis BN. Mixed-mode stress intensity factors for interacting semi-elliptical surface cracks in a plate. Eng Fract Mech 1993;45(3):357–80.
[14] Yoshimura S, Lee J-S, Yagawa G. Automated system for analyzing stress intensity factors of three-dimensional cracks: its application to analyses of two dissimilar semi-elliptical surface cracks in plate. J Press Vessel Technol Trans ASME 1997;119(1):18–26.
[15] Sethuraman R, Ilango IT. Analysis of interacting semi-elliptical surface cracks in finite thickness plates under remote bending load. Int J Press Vessels Pip 2005;82(7):528–45.
[16] Sethuraman R, Reddy GSS, Ilango IT. Finite element based evaluation of stress intensity factors for interactive semi-elliptic surface cracks. Int J Press Vessels Pip 2003;80(12):843–59.
[17] Carpinteri A, Brighenti R, Vantadori S. A numerical analysis on the interaction of twin coplanar flaws. Eng Fract Mech 2004;71(4–6):485–99.
[18] Brighenti R, Carpinteri A. Surface cracks in fatigued structural components: a review. Fatigue Fract Eng Mater Struct 2013;36(12):1209–22.
[19] Kishimoto K, Soboyejo WO, Knott JF, Smith RA. A numerical investigation of the interaction and coalescence of twin coplanar semi-elliptical fatigue cracks. Int J Fatigue 1989;11(2):91–6.
[20] Lin XB, Smith RA. Fatigue growth analysis of interacting and coalescing surface defects. Int J Fract 1997;85(3):283–99.
[21] Abaqus/CAE v6.12. Providence, RI, USA: Dassault Systemes Simulia Corp.; 2012.
[22] MATLAB®, version 8.1.0.604 (R2013a). Natick, USA: The Mathworks Inc.
[23] Abaqus/Standard v6.12. Providence, RI, USA: Dassault Systemes Simulia Corp.; 2012.
[24] Bueckner HF. Field singularities and related integral representations. In: Sih GC, editor. Methods of analysis and solutions of crack problems1. Noordhoff International; 1973. p. 239–314.
[25] Shih CF, Asaro RJ. Elastic-plastic analysis of cracks on bimaterial interfaces: Part 1-Small scale yielding. J Appl Mech Trans ASME 1988;55(2):299–316.
[26] Benthem JP. State of stress at the vertex of a quarter-infinite crack in a half-space. Int J Solids Struct 1977;13(5):479–92.
[27] Nakamura T, Parks DM. Three-dimensional stress field near the crack front of a thin elastic plate. J Appl Mech Trans ASME 1988;55(4):805–13.
[28] Raju IS, Newman JC. Stress-intensity factors for a wide range of semi-elliptical surface cracks in finite-thickness plates. Eng Fract Mech 1979;11(4):817–29.
[29] Chapuliot S. KI formula for pipes with a semi-elliptical longitudinal or circumferential, internal or external surface crack. 2000. CEA Saclay, CEA-R-5900.
[30] Fett T, Munz D. Stress intensity factors and weight functions. Computational mechanics publications. 1997.
[31] JSME S NA1–2008 codes for Nuclear Power Generation Facilities - Rules on Fitness-For-service for Nuclear Power Plants. Japanese Society of Mechanical Engineers; 2008.
[32] API 579-1 Fitness-for service, 2nd edition. Washington, DC, USA: American Petroleum Institute; 2007.
[33] GB/T 19624-2004 Safety assessment for in-service pressure vessels containing defects. Chinese National Standardization Management Committee; 2004.
[34] Dillström P, Bergman M, Brickstad B, Zang W, Sattari-Far I, Andersson P, et al. A combined deterministic and probabilistic procedure for safety assessment of components with cracks - Handbook. Strålsäkerhetsmyndigheten, SSM 2008:01; 2008.
[35] Huh N-S, Choi S, Park K-B, Kim J-M, Choi J-B, Kim Y-J. Guidance on a defect interaction effect for in-plane surface cracks using elastic finite element analyses. In: Proceedings of the ASME Pressure Vessels and Piping Division Conference, vol. 1; 2008. p. 235–41.